

# Non-Perturbative Relativistic Calculation of the Muonic Hydrogen Spectrum

J. D. Carroll\* and A. W. Thomas

*Centre for the Subatomic Structure of Matter (CSSM),  
School of Chemistry and Physics, University of Adelaide, SA 5005, Australia*

J. Rafelski

*Departments of Physics, University of Arizona, Tucson, Arizona, 85721 USA*

G. A. Miller

*University of Washington, Seattle, WA 98195-1560 USA*

(Dated: October 31, 2018)

We investigate the muonic hydrogen  $2P_{3/2}^{F=2}$  to  $2S_{1/2}^{F=1}$  transition through a precise, non-perturbative numerical solution of the Dirac equation including the finite-size Coulomb force and finite size vacuum polarization. The results are compared with earlier perturbative calculations of (primarily) Borie, Martynenko, and Pachucki [1–6]; and experimental results recently presented by Pohl *et al.* [7], in which this very comparison is interpreted as requiring a modification of the proton charge radius from that obtained in electron scattering and electronic hydrogen analyses. We find no significant discrepancy between the perturbative and non-perturbative calculations, and present our results as confirmation of the perturbative methods.

PACS numbers: 36.10.Ee, 31.30.jr, 03.65.Pm, 32.10.Fn

## I. INTRODUCTION

The precision measurement of the Lamb shift transition energy between the  $2P_{3/2}^{F=2}$  and  $2S_{1/2}^{F=1}$  states of muonic hydrogen by Pohl *et al.* [7], see Fig. 1, has created considerable interest because of a 0.31 meV discrepancy with the value predicted by theoretical calculations (specifically those discussed in Ref. [7]; Borie [1–3] and Martynenko [4, 5] along with many others [8–11]). This Lamb shift splitting of  $\mathcal{O}(206)$  meV is dominated by the lowest order QED vacuum polarization, and obtains a significant contribution from the finite size of the proton. On selecting and combining the perturbative predictions for the corresponding contributions to the measured transition, Pohl *et al.* produce a cubic equation relating their experimentally measured energy shift to the theoretical prediction, and arrive at

$$\begin{aligned} 206.2949(32) \text{ meV} &= 206.0573(45) \\ &\quad - 5.2262 \langle r_p^2 \rangle^{1/2} \\ &\quad + 0.0347 \langle r_p^2 \rangle^{3/2} \text{ meV}, \end{aligned} \quad (1)$$

the only physically-meaningful solution of which implies a proton rms charge radius of  $r_p \equiv \sqrt{\langle r_p^2 \rangle} = 0.84184(67)$  fm which differs from the consensus CODATA [12] value of  $r_p = 0.8768(69)$  fm by 4.9 standard deviations.

Such a large modification of a basic electromagnetic property of the proton suggests that either there may

be an as yet unrecognised problem in several other experimental efforts (such as the electronic hydrogen spectroscopy and scattering experiments which primarily lead to the CODATA value [12]) or in the QED calculations [13–15], or alternatively that some new physics (beyond the Standard Model) contributes to this transition energy [16–18]. With respect to the QED calculations, we note that the predominant theoretical approach involves perturbation theory applied to the solutions of the non-relativistic Schrödinger equation [1, 4, 5]. Since the effects of finite size and the vacuum polarization potential are quite large at short distance, it seems important to verify by explicit calculation that the perturbative treatment is indeed adequate at the level quoted.

We therefore calculate the transition energy relevant to the aforementioned experiment using the relativistic Dirac equation to describe the muon wave function non-perturbatively. We take care to control the numerical errors in the calculations and to quantify any differences from the perturbative non-relativistic approach. In our work we extend considerably the earlier work by Borie [1, 2].

In the sections following, we discuss the nature of the transition and contributing physical effects, as well as the method by which we calculate the energies corresponding to the various eigenstates. We summarize any discrepancies with respect to previous work.

## II. MUONIC HYDROGEN SPECTRUM

After muon capture by hydrogen, about 1% of the muons reach the metastable  $2S$ -state. This state is activated by laser excitation from  $2S_{1/2}^{F=1}$  to  $2P_{3/2}^{F=2}$  and the signature that the laser energy is well tuned is the appear-

---

\*Electronic address: jcarroll@physics.adelaide.edu.au

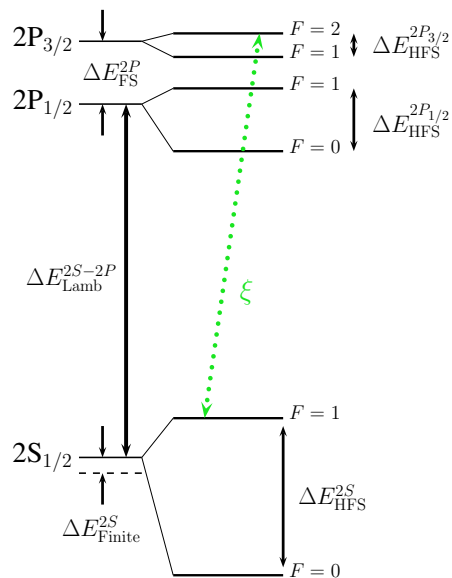


FIG. 1: (Color online) Muonic hydrogen L-shell spectrum, showing the finite proton-size correction, Lamb shift splitting, fine structure, and hyperfine structure. The  $2S_{1/2}^{F=1}$  to  $2P_{3/2}^{F=2}$  transition measured by Pohl *et al.* [7] is shown as the green dotted line (marked  $\xi$ ).

ance of a prompt E1 transition X-Ray of a muon from the  $2P_{3/2}^{F=2}$  state of muonic hydrogen to the  $1S_{1/2}^{F=1}$  state. Given the resonance method used to establish the energy of the Lamb shift, there appears to be no doubt about the remarkable experimental result of Pohl *et al.* [7].

The L-shell level scheme explored in this experiment is depicted in Fig. 1 for the point-Coulomb potential of magnitude

$$V_C(r) = -\frac{Z\alpha}{r}. \quad (2)$$

The  $2S_{1/2}$  and  $2P_{1/2}$  states are degenerate even in the Coulomb-Dirac theory. Since the muon orbit is 200 times smaller than the corresponding electron orbit, the S-states probe the point charge smearing effect of vacuum polarization, which is the dominant component in the Lamb shift,  $\Delta E_{\text{Lamb}}^{2S-2P}$ , in Fig. 1. Of similar nature is a smaller but significant effect for hydrogen ( $Z=1$ ) arising from the finite proton charge radius, denoted  $\Delta E_{\text{Finite}}^{2S}$  in Fig. 1. While the vacuum polarization effect increases the binding of the  $S_{1/2}$  states pulling these ‘down’ in Fig. 1, the finite charge distribution acts in the opposite direction.

The spin-orbit fine structure splitting of the  $2P_{1/2}$  and  $2P_{3/2}$  eigenstates is predicted by the Dirac equation. It is denoted by  $\Delta E_{\text{FS}}^{2P}$  in Fig. 1. As the measured transition does not involve the  $2P_{1/2}$  state, we shall only calculate the relevant energy levels for the purpose of comparison with perturbative results.

The spin-spin coupling of the muon to the proton adds hyperfine splitting to the spectrum. For the case of the

$2S_{1/2}$  eigenstate, this leads to hyperfine eigenstates with total angular momenta  $F=0$  and  $F=1$ . The muon involved in the measured transition decays to the  $2S_{1/2}^{F=1}$  state, and thus we address an accurate determination of the energy of this state and the corresponding splitting  $\Delta E_{\text{HFS}}^{2S}$ . Similarly, the hyperfine states are labeled by  $F=0$  and  $F=1$  for the  $2P_{1/2}$  case, and  $F=1$  and  $F=2$  for the  $2P_{3/2}$  case. The hyperfine splitting energies are denoted here by  $\Delta E_{\text{HFS}}^{2P_{1/2}}$  and  $\Delta E_{\text{HFS}}^{2P_{3/2}}$  for the corresponding states. The muon in the measured transition decays from the  $2P_{3/2}^{F=2}$  eigenstate, so we require an accurate determination of the energy of this state. We note that the muon-proton tensor force does lead to some mixing of the two  $F=1$  states but we will not make a new calculation of this effect.

### III. NUMERICAL METHOD

To calculate the theoretical energy difference corresponding to the measured transition, previous authors have primarily used perturbation theory with non-relativistic wave functions, including in the effective interaction terms describing the various relativistic corrections. In order to calculate the perturbative effect on the energy produced by an operator,  $\delta V$ , additional to the Coulomb potential,

$$V_{\text{eff}} = -\frac{Z\alpha}{r} + \delta V, \quad (3)$$

we require a wave function to integrate over. If we follow the methods of previous authors, we can use exact Schrödinger wave functions for states with quantum numbers  $n, \ell, m$  and the lowest order correction to the energy is

$$\Delta E_{\text{V}'}^{n\ell m} \approx \int_0^\infty \phi_{\text{Schröd.}}^{n\ell m \dagger}(r) \delta V \phi_{\text{Schröd.}}^{n\ell m}(r) d^3r. \quad (4)$$

An alternate approach, which we choose here, is to use the Dirac equation with the appropriate potential in order to calculate the perturbed wave functions. This approach is known to be a specific limit approximation to the two-particle Bethe-Salpeter equation [8].

We consider the muon wave function in state  $\alpha$  to be a spinor  $\psi_\alpha(\vec{r})$

$$\psi_\alpha(\vec{r}) = \begin{pmatrix} g_\alpha(r) \chi_\kappa^\mu(\hat{r}) \\ -if_\alpha(r) \chi_{-\kappa}^\mu(\hat{r}) \end{pmatrix} = \begin{pmatrix} \frac{G_\alpha(r)}{r} \chi_\kappa^\mu(\hat{r}) \\ \frac{-iF_\alpha(r)}{r} \chi_{-\kappa}^\mu(\hat{r}) \end{pmatrix}, \quad (5)$$

normalised to unity, such that the probability is

$$\int |\psi_\alpha|^2 d^3r = \int_0^\infty r^2 [g_\alpha(r)^2 + f_\alpha(r)^2] dr = 1, \quad (6)$$

noting that  $\chi_\kappa^\mu$  are eigenfunctions of the total angular momentum operator (consisting of a combination of spheri-

cal harmonics and Pauli spinors) satisfying

$$\int \chi_{\kappa}^{m\dagger} \chi_{\kappa'}^{m'} d\hat{r} = \delta_{\kappa\kappa'} \delta_{mm'}. \quad (7)$$

The separation of center of mass motion is not exact for a relativistic two body system. To lowest order in the ratio of muon to proton mass we use the reduced mass  $\mu$  in place of the muon mass in the Dirac Equation

$$\mu = \frac{M_p m_{\mu}}{M_p + m_{\mu}}. \quad (8)$$

Along with further recoil corrections treated in perturbation theory, this should provide a very accurate description of the system.

The binding of the muon in this system is extremely weak (on the scale of rest energy) and as such the eigenvalue,  $\epsilon_{\alpha}$ , for each state calculated using the Dirac equation is approximately equal to the reduced mass  $\mu$ . In order to precisely calculate the variance from this value, we rewrite the Dirac equation to incorporate the shift of eigenvalue down by the reduced mass, such that the eigenvalue we are now solving for is  $\lambda_{\alpha} = \epsilon_{\alpha} - \mu$ , corresponding to the binding energy.

The Dirac equation we wish to solve is therefore given by

$$\frac{d}{dr} \begin{pmatrix} G_{\alpha}(r) \\ F_{\alpha}(r) \end{pmatrix} = \begin{pmatrix} \frac{\kappa_{\alpha}}{r} & \lambda_{\alpha} + 2\mu - V \\ -\lambda_{\alpha} + V & \frac{\kappa_{\alpha}}{r} \end{pmatrix} \begin{pmatrix} G_{\alpha}(r) \\ F_{\alpha}(r) \end{pmatrix}, \quad (9)$$

where the value of  $\kappa_{\alpha}$  is specific to each eigenstate, namely

$$\begin{aligned} 1S_{1/2} : \kappa &= -1, & 2S_{1/2} : \kappa &= -1, \\ 2P_{1/2} : \kappa &= +1, & 2P_{3/2} : \kappa &= -2. \end{aligned}$$

In order to integrate Eq. (9), we supply an initial guess for the eigenvalue  $\lambda_{\alpha}$  and appropriate boundary conditions for the upper and lower components of the wave function at small and large radii. We then integrate from each limit towards a central matching point. The normalised discontinuity in the wave function integrated from each limit is used as a measure of the inaccuracy of the eigenvalue and a refined estimate is calculated. This process is iterated until  $\lambda_{\alpha}$  changes by less than the required tolerance.

#### IV. QUALITY CONTROL

To convince ourselves that our method is self-consistently accurate, we check the accuracy of our procedure using several methods. The unperturbed point-Coulomb Dirac eigenvalues are known analytically to be

$$\lambda_{\alpha} = \epsilon_{\alpha} - \mu = \mu \left[ 1 + \frac{Z^2 \alpha^2}{(n_{\alpha} - |\kappa_{\alpha}| + \sqrt{\kappa_{\alpha}^2 - Z^2 \alpha^2})^2} \right]^{-\frac{1}{2}} - \mu, \quad (10)$$

where  $n_{\alpha}$  denotes the principle quantum number for state  $\alpha$ . We first ensured that we are able to reproduce these values within a reasonable compute-time. For the  $2S_{1/2}$  wave function, we reproduce the analytic result to within 10 neV, the  $2P_{1/2}$  eigenstate to within 40 neV and the  $1S_{1/2}$  and  $2P_{3/2}$  eigenstates to within 10 peV, using quad-precision Fortran, a sufficiently large grid size, and sufficiently small grid spacing.

This test does not assure that solutions for a realistic case—including the finite size of the proton as well as finite size vacuum polarization—converges with same accuracy. For this reason we employ the virial theorem test for our solutions (refer to Ref. [9] for further details) by calculating the reduced eigenvalue as

$$\lambda_{\alpha} = \langle \psi_{\alpha} | \mu(\beta - 1) + V(\vec{r}) + \vec{r} \cdot \vec{\nabla} V(\vec{r}) | \psi_{\alpha} \rangle. \quad (11)$$

The virial theorem provides a far more stringent test of the accuracy of the muon wave function near the origin, where  $|\vec{\nabla} V|$  is greatest. We find that the eigenvalues calculated using Eq. (10) and Eq. (11) for the  $2S_{1/2}$  wave function differ by 180 neV for a point-Coulomb potential, and 450 neV the finite-Coulomb plus finite-vacuum polarization potentials discussed in Sec. VI. We therefore conservatively take our errors to be less than  $\pm 500$  neV. Propagating this error, we find that in principle we could determine the required proton rms charge-radius to within approximately 0.05 am ( $5 \times 10^{-5}$  fm). This should be sufficient to provide a reliable, independent test of the accuracy of the perturbative approach, however we note that the determination of the proton rms charge radius cannot be performed to this precision as the error in that analysis is dominated by experimental error in the determination of the transition energy.

#### V. $2S_{1/2}$ - $2P_{1/2}$ LAMB SHIFT

The Lamb shift is the splitting of the otherwise degenerate  $2S_{1/2}$  and  $2P_{1/2}$  eigenstates attributed to the vacuum polarization potential  $V_{VP}$ , which for a point source is given in [6] as

$$V_{VP}(r) = -\frac{Z\alpha}{r} \frac{\alpha}{3\pi} \int_4^{\infty} \frac{e^{-m_e q r}}{q^2} \sqrt{1 - \frac{4}{q^2}} \left(1 + \frac{2}{q^2}\right) dq^2, \quad (12)$$

where  $m_e$  is the electron mass. We can calculate the effect that this has on the eigenvalues by assuming that this potential is a small perturbation of the Coulomb potential, and thus using Eq. (4) we find

$$\Delta E_{\text{Lamb}}^{nlm} \approx \int_0^{\infty} V_{VP}(r) |\Psi_{\text{Schrod.}}^{nlm}(r)|^2 d^3r, \quad (13)$$

to which we must also add higher order perturbation theory, relativistic, recoil, and radiative corrections and generally higher-order (in  $\alpha$ ) corrections.

Alternatively—and more accurately—we can calculate the shift in eigenvalues using converged Dirac wave

functions in response to the combined effect of the Coulomb and vacuum polarization potentials. In this case we simply take the difference between the converged eigenvalues for the  $2S_{1/2}$  and  $2P_{1/2}$  eigenstates calculated in the presence of point-Coulomb and point-vacuum polarization potentials

$$\Delta E_{\text{Lamb}}^{2S-2P} = \lambda_{2P_{1/2}} - \lambda_{2S_{1/2}} = 205.1706(5) \text{ meV}, \quad (14)$$

Care must be taken when comparing this calculation to that of Eq. (13) since our calculation includes relativistic corrections, which are treated as corrections to Eq. (13) in Ref. [1]. A summary of this comparison and the calculated values for the Lamb shift are given in Table I, where we note that the perturbative and non-perturbative calculations are found to be in good agreement. For this table and those that follow, we refer to various iterations of our calculations in which we compute the wave function in the presence of point-Coulomb (C); finite (size nucleus)-Coulomb (FC); point vacuum polarization (VP); and finite (size nucleus) vacuum polarization (FVP) potentials. The dependence on  $\langle r_p^2 \rangle^n$  is extracted in each case by fitting the energy shifts calculated at various values of  $r_p \equiv \langle r_p^2 \rangle^{1/2}$  to a cubic of the form given in Eq. (18) for the case of a Coulomb-only potential, and with the addition of a term proportional to 1 when including the vacuum polarization (to account for the  $2S-2P$  splitting). The values listed in the column ‘Pohl *et al.*’ of Table I have their origins in references 1–5, 11, 12, 14–17, and 19–25 of Ref [7] and are taken to be reliable values.

## VI. PROTON FINITE-SIZE CORRECTIONS

The perturbative leading-order contributions associated with the finite size of the proton arise from consideration of the proton-form factor. These are introduced by Borie [3] and considered in Friar [10], Section VI below Eq. (64b). These terms appear in Pohl *et al.* [7] as quoted from Ref. [1], and are given by

$$\Delta E_{\text{Finite}} = -\frac{2Z\alpha}{3} \left( \frac{Z\alpha\mu}{2} \right)^3 \left[ \langle r_p^2 \rangle - \frac{Z\alpha\mu}{2} \langle r_p^2 \rangle^{3/2} \right]. \quad (15)$$

To calculate this effect in our fully relativistic, non-perturbative calculation, we consider the replacement of the point-Coulomb potential with the finite-size Coulomb potential in Eq. (9)

$$V_C(r) = -\frac{Z\alpha}{r} \rightarrow -Z\alpha \int \frac{\rho(r')}{|\vec{r} - \vec{r}'|} d^3r', \quad (16)$$

where  $\rho(r)$  is the proton charge-distribution (or more accurately, the Fourier transform of the Sachs electric form-factor). In response to concerns that the shape of

the form factor may significantly influence the theoretical calculations [19], we have studied the dependence of the finite-size correction on the form of this term (always normalised to unity) and this will be summarized in an upcoming publication (Ref. [20]), though the dependence on the choice of charge-distribution—whether it be exponential, Yukawa, or Gaussian in form—appears to be extremely weak.

The exponential form for the charge-distribution, normalised to unity such that  $\int \rho(r) d^3r = 1$  is given by

$$\rho(r) = \frac{\eta}{8\pi} e^{-\eta r}; \quad \eta = \sqrt{12/\langle r_p^2 \rangle}. \quad (17)$$

We calculate the Lamb shift by taking the difference between the appropriate eigenvalues calculated using the Dirac equation with the potential given by Eq. (16) with the charge-distribution given by Eq. (17) for various values of  $\langle r_p^2 \rangle$ . We then interpolate the energy shifts and fit the data to a cubic of the form

$$f(x) = A\langle r_p^2 \rangle + B\langle r_p^2 \rangle^{3/2}, \quad (18)$$

which provides the relevant parameterization. The  $\langle r_p^2 \rangle^n$  dependence in the presence of an exponential finite-sized Coulomb potential and point vacuum polarization potential

$$V(r) = -Z\alpha \int \frac{\rho(r')}{|\vec{r} - \vec{r}'|} d^3r' + V_{\text{VP}}(r), \quad (19)$$

is given by

$$\Delta E_{\text{Finite}} = 205.1706 - 5.2169\langle r_p^2 \rangle + 0.0353\langle r_p^2 \rangle^{3/2} \text{ meV}. \quad (20)$$

A further important effect of the finite size of the proton arises through the convolution of the vacuum polarization potential (Eq. (12)) with the proton charge-distribution. This leads to the replacement of the point vacuum polarization potential by

$$V_{\text{VP}}(r) \rightarrow -\frac{2Z\alpha^2}{3\pi} \int \frac{\rho(r')}{|\vec{r} - \vec{r}'|} Z_0(|\vec{r} - \vec{r}'|) d\tau', \quad (21)$$

where we use the expression given in Ref. [11]

$$Z_n(|\vec{r}'|) = \int_1^\infty e^{-\frac{\lambda}{2}|\vec{r}'|\xi} \left( 1 + \frac{1}{2\xi^2} \right) \frac{(\xi^2 - 1)^{\frac{1}{2}}}{\xi^n \xi^2} d\xi, \quad (22)$$

and where  $\lambda$  denotes the electron Compton wavelength (divided by  $2\pi$ ),  $\lambda = 386.15926459 \text{ fm}$ . When discussing this potential, it should be assumed that we are using a normalised exponential charge-distribution. We once again calculate the eigenvalues using various values of  $\langle r_p^2 \rangle$  in the charge-distribution and fit the resulting energies to a cubic (as per Eq. (18)), except that in this case the vacuum polarization induces the Lamb shift, and we must include a term proportional to 1. Thus we find

$$\Delta E_{\text{Finite}} = 205.182 - 5.2519\langle r_p^2 \rangle + 0.0546\langle r_p^2 \rangle^{3/2} \text{ meV}, \quad (23)$$

TABLE I: Contributions to the  $2S$ – $2P$  Lamb shift with comparison to values presented in Pohl *et al.* [7] which themselves are selected values from various theoretical sources—references 1–5, 11, 12, 14–17, and 19–25 of Pohl *et al.*. Values are all in meV. Errors in the Dirac calculations are taken to be  $\pm 500$  neV as per Section IV. We refer to various iterations of our calculations in which we compute the wave function in the presence of point-Coulomb (C); finite-Coulomb (FC); point vacuum polarization (VP); and finite vacuum polarization (FVP) potentials. The dependence on  $\langle r_p^2 \rangle^n$  is extracted in each case by fitting the energy shifts calculated at various values of  $r_p$  to a cubic of the form given in Eq. (18) for the case of a Coulomb-only potential, and with the addition of a term proportional to 1 when including the vacuum polarization. The listed corrections are already included in our Dirac calculations, namely lines 3 and 5 of Table 1 in Ref. [7] and the nuclear size contributions of Table 2 from that reference. All further corrections to both the perturbative calculation and our calculation are contained in ‘Remaining Corrections’ which in this case encompasses all remaining contributions of Table 1 and radiative correction of Table 2 of Ref. [7].

Contribution	Pohl <i>et al.</i>	Present Work
Dirac ( $V = V_C + V_{VP}$ )		205.1706
Dirac ( $V = V_{FC}$ )		$-5.2000 \langle r_p^2 \rangle + 0.0350 \langle r_p^2 \rangle^{3/2}$
Dirac ( $V = V_{FC} + V_{VP}$ )		$205.1706 - 5.2169 \langle r_p^2 \rangle + 0.0353 \langle r_p^2 \rangle^{3/2}$
Dirac ( $V = V_{FC} + V_{FVP}$ )		$205.1822 - 5.2519 \langle r_p^2 \rangle + 0.0546 \langle r_p^2 \rangle^{3/2}$
Relativistic one loop VP	205.0282	
Polarization insertion in two Coulomb lines	0.1509	
Finite size effects	$-5.1987 \langle r_p^2 \rangle + 0.0347 \langle r_p^2 \rangle^{3/2}$	
Subtotal:	$205.1791 - 5.1987 \langle r_p^2 \rangle + 0.0347 \langle r_p^2 \rangle^{3/2}$	$205.1822 - 5.2519 \langle r_p^2 \rangle + 0.0546 \langle r_p^2 \rangle^{3/2}$
Remaining Corrections		$0.8782 - 0.0275 \langle r_p^2 \rangle$
Total:	$206.0573 - 5.2262 \langle r_p^2 \rangle + 0.0347 \langle r_p^2 \rangle^{3/2}$	$206.0604 - 5.2794 \langle r_p^2 \rangle + 0.0546 \langle r_p^2 \rangle^{3/2}$

which is the expression which is compared to the perturbative calculation in Table I. We note that the finite-vacuum polarization induces a small but non-trivial shift, and that the results are otherwise essentially the same as those of Pohl *et al.* [7].

## VII. $2P$ FINE STRUCTURE

The  $\mathcal{O}(Z\alpha)^4$  perturbative  $2P$  fine structure splitting is calculated in Ref. [5] to be

$$\Delta E_{FS}^{2P} = \frac{\mu^3 (Z\alpha)^4}{32m_\mu^2} \left( 1 + \frac{2m_\mu}{m_p} \right), \quad (24)$$

along with higher-order corrections. Taking this splitting as the difference between the converged eigenvalues of the  $2P_{1/2}$  and  $2P_{3/2}$  eigenstates gives

$$\Delta E_{FS}^{2P} = \lambda_{2P_{3/2}} - \lambda_{2P_{1/2}}, \quad (25)$$

which we can also calculate in the presence of the various potentials. For the case of an exponential finite-Coulomb potential with finite vacuum polarization, the  $2P$  fine structure splitting is

$$\Delta E_{FS}^{2P} = 8.4206(5) \text{ meV}. \quad (26)$$

A comparison of this value with perturbative calculations of Borie [1] is presented in Table II. The effect of the

finite-size Coulomb potential (as compared to the point case) is negligible at the level of errors of our calculation. Similarly, the effect of the finite-size vacuum polarization is also negligible at our level of errors. The vacuum polarization itself increases the fine structure splitting by  $5 \mu\text{eV}$ . We note that the perturbative and non-perturbative calculations are in perfect agreement to the level of errors presented here.

## VIII. HYPERFINE STRUCTURE

The hyperfine structure is a measure of the  $\vec{\ell} \cdot \vec{\sigma}$  coupling. Following the lead of Ref. [21], the appropriate Hamiltonian is given by

$$\mathcal{H} = 2\beta_\mu \gamma \hbar \frac{\ell(\ell+1)}{j(j+1)} \left\langle \frac{1}{r^3} \right\rangle \mathbf{I} \cdot \mathbf{J} + \frac{16\pi}{3} \beta \gamma \hbar |\psi(0)|^2 \mathbf{I} \cdot \mathbf{S}, \quad (27)$$

comprising a dipole term and a contact term, for which the following definitions apply for the muon Bohr magneton  $\beta_\mu$ ; proton Bohr magneton  $\beta_p$ ; and proton gyromagnetic ratio  $\gamma$

$$\beta_\mu = \sqrt{\alpha}/2m_\mu, \quad \beta_p = \sqrt{\alpha}/2M_p, \quad \gamma = 2(1 + \kappa)\beta_p. \quad (28)$$

Here  $\kappa = 1.792847351$  is the proton anomalous magnetic moment.  $\psi(0)$  represents the muon wave function at the

TABLE II: Contributions to the  $2P$  fine-structure splitting with comparison to values found in Borie [1]. Subscripts are defined in Table I. Values are all in meV. Errors in the Dirac calculations are taken to be  $\pm 500$  neV as per Section IV. The listed correction (Uehling/vacuum polarization) is already included in our Dirac calculations. All further corrections to both the perturbative calculation and our calculation are contained in ‘Remaining Corrections’ which are detailed in Table II of Ref. [1]. Finite-size effects in either the Coulomb or vacuum polarization potentials provide no shift above the level of errors here, as expected for P-states. The perturbative calculation prediction is reproduced within errors.

Contribution	Borie	Present Work
Dirac ( $V = V_C$ )	8.4156	8.4156
Dirac ( $V = V_{FC}$ )		8.4156
Dirac ( $V = V_C + V_{VP}$ )		8.4206
Dirac ( $V = V_{FC} + V_{VP}$ )		8.4206
Dirac ( $V = V_{FC} + V_{FVP}$ )		8.4206
Uehling (VP)	0.0050	
Subtotal	8.4206	8.4206
Remaining Corrections	-0.06852	
Total:	8.3521	8.3521

centre of the proton. We now investigate the two terms of Eq. (27) separately.

### A. $2S_{1/2}$ Hyperfine Structure

There exist several methods by which the  $2S$  hyperfine structure can be calculated. The perturbative  $2S$  hyperfine structure calculated in Ref. [4] is given by

$$\Delta E_{HFS}^{2S_{1/2}} = \frac{1}{3}(Z\alpha)^4 \frac{\mu^3}{m_\mu m_p} (1 + \kappa). \quad (29)$$

For  $\ell = 0$  the contact term in the Hamiltonian (Eq. (27)) is non-zero, while the dipole term vanishes;

$$E_{HFS}^{2S} = \frac{16\pi}{3} \beta_\mu \gamma \hbar |\psi(0)|^2 \langle F m_F | \mathbf{I} \cdot \mathbf{S} | F m_F \rangle, \quad (30)$$

where  $|F m_F\rangle$  is the eigenfunction belonging to  $\mathbf{F} = \mathbf{I} + \mathbf{J}$ , such that

$$\langle F m_F | \mathbf{I} \cdot \mathbf{S} | F m_F \rangle = \frac{1}{2} \left[ F(F+1) - \frac{3}{2} \right]. \quad (31)$$

Thus, the splitting between the  $2S$   $F = 0$  and  $F = 1$  hyperfine levels is given by

$$\Delta E_{HFS}^{2S(F=1-F=0)} = \frac{16\pi}{3} \beta_\mu \gamma \hbar |\psi(0)|^2, \quad (32)$$

We note an important, relevant typographical correction; In Ref. [21] Eq. (18.2-17b), the sign should be positive and the second 9 in the denominator should not appear.

The value of the  $2S$  hyperfine splitting, as calculated using Eq. (32) with the wave function calculated with the Dirac equation in the presence of the combined exponential finite-Coulomb and finite vacuum polarization potentials is

$$\Delta E_{HFS}^{2S} = 22.7690(5) \text{ meV}. \quad (33)$$

We note that the effect of including the exponential finite-size Coulomb potential as compared to the point case reduces the splitting by  $0.1269(5)$  meV; introducing the point vacuum polarization potential increases the splitting by  $0.0747(5)$  meV for the point-Coulomb, and  $0.0742(5)$  meV for the finite-Coulomb cases. Using the combined finite vacuum polarization and finite-Coulomb potentials reduces the splitting by  $0.0012(5)$  meV to give the value above.

Alternatively, one can follow Ref. [2] in which case we can calculate this splitting to be

$$\Delta E_{HFS}^{2S} = \frac{\kappa g \mu}{\kappa^2 - \frac{1}{4}} [\Lambda(\Lambda + 1) - I(I + 1) - j(j + 1)] \times \frac{\alpha}{2M_p} \int r^{-2} g(r) f(r) dr. \quad (34)$$

In that case, we calculate

$$\Delta E_{HFS}^{2S} = 22.7640(5) \text{ meV}, \quad (35)$$

provided we correct for the reduced mass in the formula such that the magnetic moment of the muon is not defined in terms of reduced mass but rather defined in terms of the free space mass.

A comparison to perturbative calculations is given in Table III, where we note the finding of a finite-size dependent contribution in this splitting, which is neglected in the summary of Pohl *et al.* (though finite-size effects sans a parameterization are calculated in studies by Borie [1] and Pachucki [6]) and which differs from results obtained using the standard Zemach treatment [6]. We note that for  $\langle r_p^2 \rangle^{1/2} = 0.8768$  fm, the  $2S_{1/2}$  hyperfine splitting is calculated here to be 22.8496 meV (22.8547 meV for  $\langle r_p^2 \rangle^{1/2} = 0.84184$  fm) which indicates a  $0.0087(5)$  meV ( $0.0100(5)$  meV) correction to the perturbative calculation (once the factor of  $1/4$  is taken into account), or  $2.8$ – $3.2\%$  of the  $0.31$  meV quoted discrepancy.

### B. $2P_{1/2}$ Hyperfine Structure

The  $2P_{1/2}$  hyperfine structure is of no consequence for the transition which we are investigating here. Nonetheless, we calculate the energy of the  $2P_{1/2}^{F=0}$  and  $2P_{1/2}^{F=1}$  levels as a confirmation of our method, and to compare to the perturbative results. Following Ref. [5], to  $\mathcal{O}(\alpha^4)$  the  $2P_{1/2}$  hyperfine structure splitting is given by

$$\Delta E_{HFS}^{2P_{1/2}} = E_F \left[ \frac{1}{3} + \frac{a_\mu}{6} + \frac{m_\mu(1 + 2\kappa)}{12m_p(1 + \kappa)} \right], \quad (36)$$

TABLE III: Contributions to the  $2S_{1/2}$  hyperfine splitting calculated via Eq. (32) with comparison to values found in Martynenko [4]. Subscripts are defined in Table I. Values are all in meV. Errors in the Dirac calculations are taken to be  $\pm 500$  neV as per Section IV. The listed corrections are already included in our Dirac calculations and are listed by their descriptions in Ref. [4]. All further corrections to both the perturbative calculation and our calculation are contained in ‘Remaining Corrections’ which encompasses the muon AMM, amongst other corrections listed in Ref. [4]. We note that the ‘Proton structure corrections of  $\mathcal{O}(\alpha^5)$ ’ pertains to the Zemach contribution (which we shall explore in an upcoming publication) and does not include considerations of finite-size in the wavefunction, and that the polynomial dependence on  $\langle r_p^2 \rangle^n$  of this splitting is not discussed in the literature.

Contribution	Martynenko	Present Work
Dirac ( $V = V_C$ )		22.8229
Dirac ( $V = V_C + V_{VP}$ )		22.8976
Dirac ( $V = V_{FC}$ )		$22.7774 - 0.1746 \langle r_p^2 \rangle + 0.0709 \langle r_p^2 \rangle^{3/2}$
Dirac ( $V = V_{FC} + V_{VP}$ )		$22.8510 - 0.1701 \langle r_p^2 \rangle + 0.0667 \langle r_p^2 \rangle^{3/2}$
Dirac ( $V = V_{FC} + V_{FVP}$ )		$22.8521 - 0.1795 \langle r_p^2 \rangle + 0.0739 \langle r_p^2 \rangle^{3/2}$
Fermi Energy $E_F$	22.8054	
Relativistic correction $\frac{17}{8}(Z\alpha)^2 E_F$	0.0026	
VP corrections of orders $\alpha^5, \alpha^6$ in the second order of perturbation series	0.0746	
Proton structure corrections of order $\alpha^5$	-0.1518	
Proton structure corrections of order $\alpha^6$	-0.0017	
Subtotal:	22.7291	$22.8521 - 0.1795 \langle r_p^2 \rangle + 0.0739 \langle r_p^2 \rangle^{3/2}$
Remaining Corrections		0.0857
Total:	22.8148	$22.9378 - 0.1795 \langle r_p^2 \rangle + 0.0739 \langle r_p^2 \rangle^{3/2}$

for which the Fermi energy is

$$E_F = \frac{\mu^3(1 + \kappa)}{3m_\mu m_p} (Z\alpha)^4, \quad (37)$$

and where  $\alpha_\mu$  is the muon anomalous magnetic moment. We note another important, relevant typographical correction; in Ref. [5] the factors of 2 in the denominators of the third terms of Eqs. (27–28) should read 12. The calculations are performed correctly however. For  $\ell \neq 0$ , the dipole term in the Hamiltonian (Eq. (27)) is non-zero, while the contact term vanishes. The energy for the dipole term is thus given by

$$E_{\text{HFS}}^{2P_{1/2}} = 2\beta\gamma\hbar \frac{\ell(\ell+1)}{j(j+1)} \left\langle \frac{1}{r^3} \right\rangle \langle Fm_F | \mathbf{I} \cdot \mathbf{J} | Fm_F \rangle, \quad (38)$$

where the non-zero terms in the dot-product are given by

$$\langle Fm_F | \mathbf{I} \cdot \mathbf{J} | Fm_F \rangle = \frac{1}{2} [F(F+1) - I(I+1) - j(j+1)]. \quad (39)$$

For Schrödinger wave functions, the vacuum expectation value of  $r^{-3}$  is analytic, in that

$$\left\langle \frac{1}{r^3} \right\rangle = \left( a_0^3 n^3 \ell(\ell+1) \left( \ell + \frac{1}{2} \right) \right)^{-1}. \quad (40)$$

Inserting the appropriate values of  $F, n, \ell, I, j$  for each of the  $F = 0$  and  $F = 1$  states, one obtains the energy of the  $2P_{1/2}$  hyperfine structure to be

$$\Delta E_{\text{HFS}}^{2P_{1/2}} = \frac{2}{9} \beta\gamma\hbar/a_0^3. \quad (41)$$

Eq. (41) corresponds to the leading term of Eq. (36), to which the anomalous magnetic moments provide additional corrections. Using the converged Dirac wave functions with exponential finite-Coulomb and finite vacuum polarization potentials (rather than Schrödinger wave functions) we calculate the expectation value of  $r^{-3}$  and find

$$\Delta E_{\text{HFS}}^{2P_{1/2}} = 7.6204(5) \text{ meV}. \quad (42)$$

The results of this calculation are summarised in Table IV where we note that the addition of the (point) vacuum polarization potential to the point-Coulomb potential increases the splitting by 0.0017(5) meV, and the introduction of the finite-Coulomb potential increases this further by 0.0045(5) meV to arrive at the value above. The effect of finite-vacuum polarization is essentially zero here.

### C. $2P_{3/2}$ Hyperfine Structure

Following the same method as in the previous subsection, we can calculate the energy levels for the  $2P_{3/2}^{F=1}$  and

TABLE IV: Contributions to the  $2P_{1/2}$  hyperfine splitting with comparison to values found in Martynenko [5]. Subscripts are defined in Table I. Values are all in meV. Errors in the Dirac calculations are taken to be  $\pm 500$  neV as per Section IV. The listed corrections are already included in our Dirac calculations. The ‘Leading contribution’ is extracted from the  $\mathcal{O}(Z\alpha)^4$  line in Table II of Ref. [5] and includes only the  $E_F/3$  term of Eq. (36). The relativistic correction is listed as  $\mathcal{O}(Z\alpha)^6$  in that reference. All further corrections to both the perturbative calculation and our calculation are contained in ‘Remaining Corrections’ which encompasses the muon AMM, proton MM, and all other lines of Table II in Ref. [5] not already listed. We note the minor error in the last digit of the summary contribution of Ref. [5] for this state, likely arising from round-off error.

Contribution	Martynenko	Present Work
Dirac ( $V = V_C$ )		7.6141
Dirac ( $V = V_C + V_{\text{VP}}$ )		7.6159
Dirac ( $V = V_{\text{FC}} + V_{\text{VP}}$ )		7.6204
Dirac ( $V = V_{\text{FC}} + V_{\text{FVP}}$ )		7.6204
Leading contribution	7.6018	
$\mathcal{O}(Z\alpha)^6$ contribution	0.0011	
Subtotal	7.6029	7.6204
Remaining Corrections		0.3615
Total:	7.9644	7.9819

$2P_{3/2}^{F=2}$  levels. The  $2P_{3/2}$  hyperfine structure, as derived in Ref. [5] is given by

$$\Delta E_{\text{HFS}}^{2P_{3/2}} = E_F \left[ \frac{2}{15} - \frac{a_\mu}{30} + \frac{m_\mu(1 + 2\kappa)}{12m_p(1 + \kappa)} \right], \quad (43)$$

where  $E_F$  is given in Eq. (37) (we note again the typographical correction detailed in Section VIII B). Alternatively, inserting the relevant values for this state into Eq. (39) and using the converged Dirac wave functions we find

$$\Delta E_{\text{HFS}}^{2P_{3/2}} = 3.0415(5) \text{ meV} \quad (44)$$

when the potential consists of the exponential finite-Coulomb and point vacuum polarization potentials. For this state, the addition of the (point) vacuum polarization potential to the point-Coulomb potential increases the splitting by 0.0007(5) meV to the value listed in Table V, and the introduction of the finite-Coulomb potential was found to have no effect within the limits of our calculation, so too was the introduction of the finite vacuum polarization potential.



TABLE V: Contributions to the  $2P_{3/2}$  hyperfine splitting with comparison to values found in Martynenko [5]. Subscripts are defined in Table I. Values are all in meV. Errors in the Dirac calculations are taken to be  $\pm 500$  neV as per Section IV. The details of the listed corrections are the same as those of Table IV.

Contribution	Martynenko	Present Work
Dirac ( $V = V_C$ )		3.0408
Dirac ( $V = V_C + V_{VP}$ )		3.0415
Dirac ( $V = V_{FC} + V_{VP}$ )		3.0415
Dirac ( $V = V_{FC} + V_{FVP}$ )		3.0415
Leading contribution	3.0407	
Relativistic correction	0.0001	
Subtotal	3.0408	3.0415
Remaining Corrections		0.3518
Total:	3.3926	3.3933

## IX. SUMMARY

We summarise the findings of these non-perturbative Dirac calculations and compare to the previous literature values of perturbative calculations in Table VI. We add to this a combined expression for the cubic which when set equal to the experimental value of the measured transition is solved to predict the proton rms charge-radius, as is done in Ref. [7].

We do not include the result of hyperfine splitting calculations for the  $2P_{1/2}$  eigenstate as this is of no relevance to the measured transition. We also note the omission here of the energy shift attributed to a mixing between the  $2P_{1/2}$  and  $2P_{3/2}$   $F = 1$  states, as discussed in Ref. [6] for comparison to Ref. [7] where it is also absent.

We find that the perturbative calculations are largely reproduced using our methods when considering the appropriate potentials for comparison. We further find that in several cases the use of the finite-vacuum polarization potential produces effects which are not accounted for in previous studies. The largest of these is the finite-size contribution to the  $2S_{1/2}$  hyperfine splitting which has been neglected in the literature up to this point.

Overall, the non-perturbative calculations do not elucidate any missing contributions of a magnitude large enough to resolve the proton radius problem outlined in Pohl *et al.* [7].

## X. CONCLUSIONS

After careful consideration of the various contributions to the measured transition energy of Pohl *et al.* [7], cal-

culated consistently using the Dirac equation with appropriate potentials, and following the addition of the required corrections to these calculations (taking further care to avoid overcounting issues), we find no single term which leads to a discrepancy with the perturbative results of sufficient magnitude to account for the discrepancy reported in Ref. [7]. These calculations nonetheless provide a useful insight into the reliability of the perturbative calculations, and allow a simpler approach to future investigations.

While it remains possible in principle that one or more of the higher-order corrections to the terms calculated in this work might be of sufficient magnitude to affect the analysis of Ref. [7], the precision with which the Dirac and perturbative calculations agree for the terms which we have calculated here strongly suggests that this will not be the case.

In addition to the calculations presented here, we further note that our calculations of a hitherto overlooked contribution arising from off-mass-shell effects for the proton (which are negligible for electronic hydrogen) provide a natural solution to the proton radius problem [13], and as such the combination of these two sets of calculations may be seen as a complete description of the measured transition in muonic hydrogen with no discrepancy in the rms charge radius of the proton. Because of the uncertain magnitude of the off-mass-shell effects, it is incorrect to complete the analysis of this transition to predict a proton rms charge radius—we await the results of current and future experiments which will be ascertain the strength of this contribution, after which a complete analysis will be possible.

Nonetheless, we note that our calculations predict that the transition energy for the  $2P_{3/2}^{F=2}$  to  $2S_{1/2}^{F=1}$  transition in muonic hydrogen is larger in magnitude than that which is predicted by the perturbative calculations, and that analysis of this data under the assumption that no further terms are required leads to the following values for the proton rms charge radius when fit to the experimental data;

$$\text{Pohl } et al. : \quad \sqrt{\langle r_p^2 \rangle} = 0.84183(67) \text{ fm},$$

$$\text{Present Work} : \quad \sqrt{\langle r_p^2 \rangle} = 0.83811(67) \text{ fm}.$$

The value listed as Present Work is taken as the solution to the cubic equation

$$209.9505 - 5.2345\langle r_p^2 \rangle + 0.0361\langle r_p^2 \rangle^{3/2} = 206.2949, \quad (45)$$

where the right-hand-side corresponds to the quoted value of the measured transition in Ref. [7]; the left-hand-side is taken from the relevant conclusion line of Table VI; and for which the errors in this calculation are dominated by the experimental error. The extracted  $\sqrt{\langle r_p^2 \rangle}$  value listed as Pohl *et al.* is taken from Ref. [7] (calculated in the same fashion) and differs from the central value

TABLE VI: Sum of perturbative and non-perturbative theoretical contributions to the measured experimental transition energy shown in Fig. 1. Subscripts are defined in Table I. Values are all in meV. The individual perturbative contributions (listed under ‘Various’) are taken from Tables I–V. In each case, the value given for the Dirac calculation is calculated using the combination of finite-Coulomb and finite vacuum polarization potentials ( $V = V_{\text{FC}} + V_{\text{FVP}}$ ). The fractional factors for the hyperfine splittings are inserted for relevance to the measured transition, and are calculated via angular-momentum splitting rules.

Contribution	Various	Present Work
$2S_{1/2}$ - $2P_{1/2}$ Lamb shift (constant)	206.0573	206.0604
$2S_{1/2}$ - $2P_{1/2}$ Lamb shift (finite-size)	$-5.2262\langle r_p^2 \rangle + 0.0347\langle r_p^2 \rangle^{3/2}$	$-5.2794\langle r_p^2 \rangle + 0.0546\langle r_p^2 \rangle^{3/2}$
$2P$ Fine Structure	8.3521	8.3521
$\frac{1}{4} \times 2S_{1/2}$ Hyperfine (constant)	-5.7037	-5.7345
$\frac{1}{4} \times 2S_{1/2}$ Hyperfine (finite-size)	0.0000	$0.0449 \langle r_p^2 \rangle - 0.0185 \langle r_p^2 \rangle^{3/2}$
$\frac{3}{8} \times 2P_{3/2}$ Hyperfine	1.2722	1.2725
<b>(Various) Total (Perturbative)</b>	<b>209.9779 - 5.2262 <math>\langle r_p^2 \rangle + 0.0347 \langle r_p^2 \rangle^{3/2}</math></b>	
<b>(Present Work) Total (Dirac)</b>	<b>209.9505 - 5.2345 <math>\langle r_p^2 \rangle + 0.0361 \langle r_p^2 \rangle^{3/2}</math></b>	

quoted in [7]; 0.84184(67), though the difference is well within the quoted errors.

We note the degree to which the cubic expression Eq. (45) agrees with that of Ref. [7], despite the latter not involving a calculation of a finite-size contribution to the  $2S$  hyperfine splitting. Some research in progress by the authors will elucidate some further overlooked contributions that will likely alter the agreement between these two expressions, and we look forward to future measurements with which we may compare our findings.

### Acknowledgments

This research was supported in part by the United States Department of Energy (under which Jefferson Sci-

ence Associates, LLC, operates Jefferson Lab) via contract DE-AC05-06OR23177 (JDC, in part); grant FG02-97ER41014 (GAM); and grant DE-FG02-04ER41318 (JR), and by the Australian Research Council (through grant FL0992247) and the University of Adelaide (JDC, AWT). GAM and JR gratefully acknowledge the support and hospitality of the University of Adelaide while the project was undertaken. The authors thank R. Pohl, E. Borie, and F. Kottmann for their comments and corrections of numerical and typographical errors.

- 
- [1] E. Borie, Phys. Rev. A **71**, 032508 (2005), physics/0410051.
- [2] E. Borie and G. A. Rinker, Rev. Mod. Phys. **54**, 67 (1982).
- [3] E. Borie, Z. Phys. **A275**, 347 (1975).
- [4] A. Martynenko, Phys.Rev. **A71**, 022506 (2005), hep-ph/0409107.
- [5] A. Martynenko, Phys.Atom.Nucl. **71**, 125 (2008), hep-ph/0610226.
- [6] K. Pachucki, Phys.Rev. **A53**, 2092 (1996).
- [7] R. Pohl, A. Antognini, F. Nez, F. D. Amaro, F. Biraben, et al., Nature (and Supplementary Material) **466**, 213 (2010).
- [8] M. I. Eides, H. Grotch, and V. A. Shelyuto, Phys. Rept. **342**, 63 (2001), hep-ph/0002158.
- [9] J. Rafelski, Phys. Rev. **D16**, 1890 (1977).
- [10] J. L. Friar, Ann. Phys. **122**, 151 (1979).
- [11] B. Fricke, Z. Phys. **218**, 495 (1969).
- [12] P. J. Mohr, B. N. Taylor, and D. B. Newell, Rev. Mod. Phys. **80**, 633 (2008), 0801.0028.
- [13] G. A. Miller, A. W. Thomas, J. D. Carroll, and J. Rafelski (2011), 1101.4073.
- [14] R. J. Hill and G. Paz (2011), 1103.4617.
- [15] I. C. Cloet and G. A. Miller, Phys.Rev. **C83**, 012201 (2011), 1008.4345.
- [16] D. Tucker-Smith and I. Yavin (2010), 1011.4922.
- [17] J. Jaeckel and S. Roy (2010), 1011.0692.
- [18] B. Batell, D. McKeen, and M. Pospelov (2011), 1103.0721.
- [19] A. De Rujula, Phys. Lett. **B697**, 26 (2011), 1010.3421.
- [20] J. Carroll, A. Thomas, J. Rafelski, and G. Miller (2011), (in preparation), 1108.2541.
- [21] M. Weissbluth, *Atoms and molecules* (Academic Press, 1978), ISBN 9780127444505.